FULL PAPER DOI: 10.1002/adsc.202001349

Advanced Synthesis & Catalysis

Very Important Publication

Unraveling the C–H Arylation of Benzo-Fused Cycloalkanones: Combined Experimental and Computational Evidence

Benjamin Large[a] and Damien Prim[a,*]

[a] Université Paris-Saclay, UVSQ, CNRS, Institut Lavoisier de Versailles, 78035, Versailles, France
E-mail: damien.prim@uvsq.fr

Manuscript received: October 31, 2020; Revised manuscript received: January 12, 2021;
Version of record online: Februar 1, 2021

Supporting information for this article is available on the WWW under https://doi.org/10.1002/adsc.202001349

Abstract: The C–H functionalization of benzo-fused cycloalkanones represents a synthetic challenge, since such scaffolds display different activation sites, at sp^2 and sp^3 carbons, a bicyclic structure, and various sizes of the cycloalkanone ring. Anticipating the outcome of C–H functionalization and the impact of the presence and size of the cycloalkanone ring would help to foresee synthetic routes to more complex molecular architectures. The mechanism of C–H arylation was studied using DFT calculations for tetralone, benzosuberone, and indanone and compared to acetophenone. Comparison of energetic profiles allowed identifying key steps of the process. Analysis of the topology of key intermediates allowed correlating the deformation of palladacycles to the potential reactivity of the benzo-fused cycloalkanone family members. The experimental results were in full agreement with the trend provided by the theoretical study. A wide panel of diversely substituted benzo-fused cycloalkanones has been successfully obtained using optimized conditions. Moreover, an approach towards polycyclic molecules has been illustrated featuring a C–H arylation and a second step taking advantage of the remaining ketone fragment and its ability to undergo diverse transformations leading to alternative pathways to more complex molecular architectures

Keywords: Tetralone; benzosuberone; indanone; C–H functionalization; Transient directing group

Introduction

The functionalization of aromatic rings by selective activation of C–H bonds has experienced an unprecedented growth allowing the construction of elaborate molecular architectures and the late stage installation of substituents.[1–10] Although C–H activation has become a powerful synthetic tool to construct new C–C or C-heteroatom bonds, and despite recent advances in the development of directing groups (DG), site selection remains a significant challenge in polycyclic substrates. The latter combine structural, electronic and steric effects within the same architecture. Thus, understanding the origin and/or predicting the selectivity of reactions using such DG requires gaining insights though related precursors or models and/or combining experimental and computational methods. Among bicyclic architectures, the benzo-fused cycloalkanone series represents a challenging family of substrates displaying different activation sites (sp^2 and sp^3 carbons), a bicyclic benzo-annulated core, a reactive carbonyl fragment and a partially hydrogenated ring of various sizes.

Such structural features are likely to hamper the transposition of catalytic systems from simplest substrates to related homologues. Indeed, in the acetophenone (and benzaldehyde) series, Pd- and Ru-promoted C_{sp2}–H as well as Pd-catalyzed C_{sp3}–H functionalizations are well documented and high yielding transformations.[11–18] (Figure 1)

In contrast, C_{sp2}–H functionalization of tetralone is almost exclusively described using Ru catalysis. If palladium-based catalytic systems efficiently promote C_{sp3}–H functionalization,[18] examples of C_{sp2}–H functionalization of tetralone using a transient directing group are scarce. In fact, C–H functionalization of benzo-fused cycloalkanones remains an underexplored transformation only exemplified with few or rare examples of arylated tetralones[19–22] and benzosuberones[21,23,24] and restricted to aromatics bear-

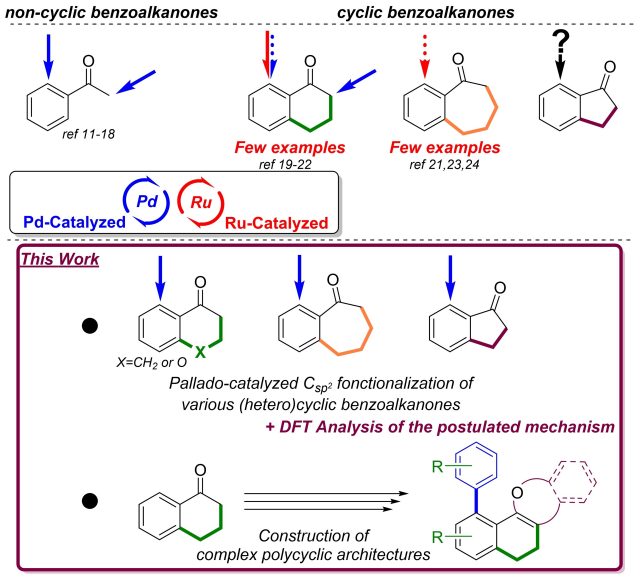

Figure 1. Acetophenone and alkanone functionalization sites and catalytic systems.

ing electron withdrawing groups. In addition, the arylation of indanone has not been studied so far.

General strategies allowing the selective installation of substituents on benzo-fused cycloalkanones are of current interest. Indeed, tetralones, indanones and benzosuberones, are important bicyclic scaffolds widely spread in natural products and display a broad array of biological properties. Further, as tetralones are considered as direct precursors of naphthalene derivatives,[25–29] the selective functionalization of tetralone platform might (i) represent an alternative route to diversely substituted naphthalenes.[30–33] (ii) allow the modulation of the substitution pattern and thus, of the properties of naphthalene derivatives in materials and life science issues.[34,35] (iii) overcome current hurdles in C–H activation chemistry of naphthalene towards 1,2,8-trisubstituted naphthalenes for examples.[36–38]

In this context, bare and fragmentary experimental and theoretical data available in the C–H functionalization of benzo-fused cycloalkanones, prompted us to examine the C–H arylation of such substrates. Our approach foresee the use of a transient directing groups (tDG)[39–41] to promote the regioselective $C_{\alpha,sp2}$–H bond activation of benzo-fused cycloalkanones and to take benefit from the intact ketone fragment to construct polycyclic architectures. We first examined the impact of the presence and the size of the condensed cycloalkanone ring on the main key steps and intermediates of the mechanism of the $C_{\alpha,sp2}$–H bond activation sequence by mean of theoretical calculations. The energetic profiles of the Pd-catalyzed arylation process of cyclic tetralone, indanone and suberone have been determined and compared to acyclic acetophenone. The reactivity trend within this series was confirmed by experimental results and illustrated by the synthesis of a broad family of aryl-benzo-cycloalkanones. Next, our strategy towards polycyclic architectures from the residual ketone fragment was also exemplified in the tetrahydro-naphthalene and the naphthalene series.

Results and Discussion

DFT Study

We based our approach on the premise plausible mechanism postulated by Jin in a recent paper dealing with the arylation of acetophenone.[17] In the context of the cornerstone tetralone substrate, key steps of this mechanism (Scheme 1) could successively involve the formation of the tDG (**A**), the coordination of the metal (**B**), C–H activation (**C**), oxidative addition (**D**), reductive elimination (**E**), regeneration of the catalytic active species (**F**) and finally regeneration of the tDG (**G**).

Considering these steps, we first determined the optimal energetic profile for the arylation of tetralone (full details are given in the ESI). As shown in Figure 2, the coordination/C–H bond activation sequence is the first key issue of the mechanism. If coordination of the Pd can be envisioned from both *Z* and *E* imine of the tDG, calculations allowed a clear discrimination between pathways involving intermediates **INT2*E*.18*E*** or **INT2*E*.18*Z*** (Figure 2).

Notably, C–H activation step **C** is assumed to proceed through carboxylate assisted CMD mechanism

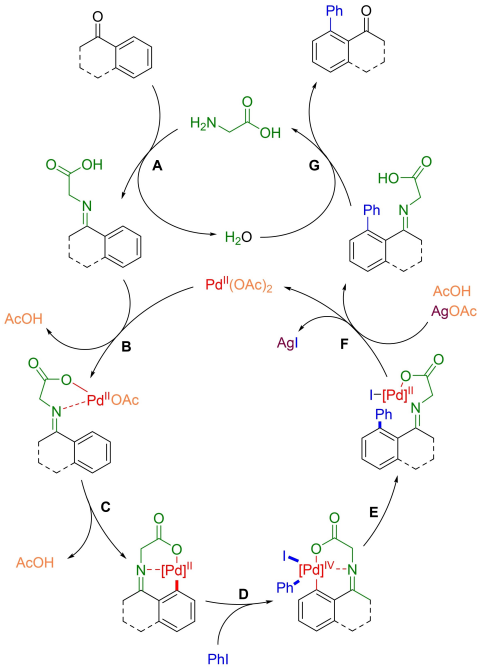

Scheme 1. Jin's postulated mechanism.

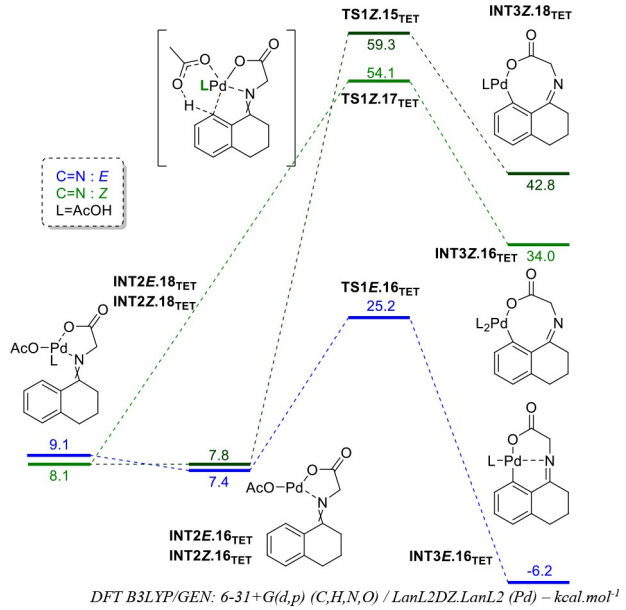

Figure 2. Energetics of reaction coordinates for step C with the starting material (benzo-fused cycloalkanone) as reference (0 kcal.mol^{-1}).

via **TS1**. Access to either **INT3*Z*.18** or **INT3*Z*.16** via **TS1*Z*.15** or **TS1*Z*.17** arising from the Z imine (barriers of 51.5 and 46.0 kcal.mol^{-1} respectively) are both strongly disfavored by comparison with the access to **INT3*E*.16** via **TS1*E*.16** (barrier of 17.8 kcal.mol^{-1}) arising from the *E* imine. Since intermediate **INT3** arising from the *E* imine is also thermodynamically favored, by comparison with the *Z* imines analogues, the overall *Z* path was not discussed further in the paper and only **INT3*E*** was considered for the next steps (the full calculated *Z* profile can be found in ESI).

The following main mechanistic steps involve the oxidative addition of aryl iodide (step **D** via **TS2*E***) followed by reductive elimination (step **E** via **TS3*E***) finally leading to the formation of a C–C bond at position 8 of the tetralone platform (Figure 3). The key intermediate **INT5*E*.18** can by plausibly obtained from two alternative pathways via **TS2*E*.16** or **TS2*E*.18** which only differ by the association/dissociation of ligand L sequence from **INT3*E*.16**. Similarly, the reductive elimination step leading to **INT6*E*.16** could occur directly from **TS3*E*.17** or via **TS3*E*.15** and **INT6*E*.14**. Finally, **INT6*E*.16** generates the expected product (**Prod**) after release of the tDG and regeneration of the catalytic active species (steps **F** and **G**). Including the dispersion in these calculations revealed that the associative pathways (in green) could be slightly favored against the dissociative ones (in blue). This difference may suggest some uncertainty in the exact mechanistic pathway (Figure 4).

The same approach was next applied to acetophenone on one hand and to benzosuberone and indanone on another hand. In all cases energetic profiles have been determined allowing the comparison of the

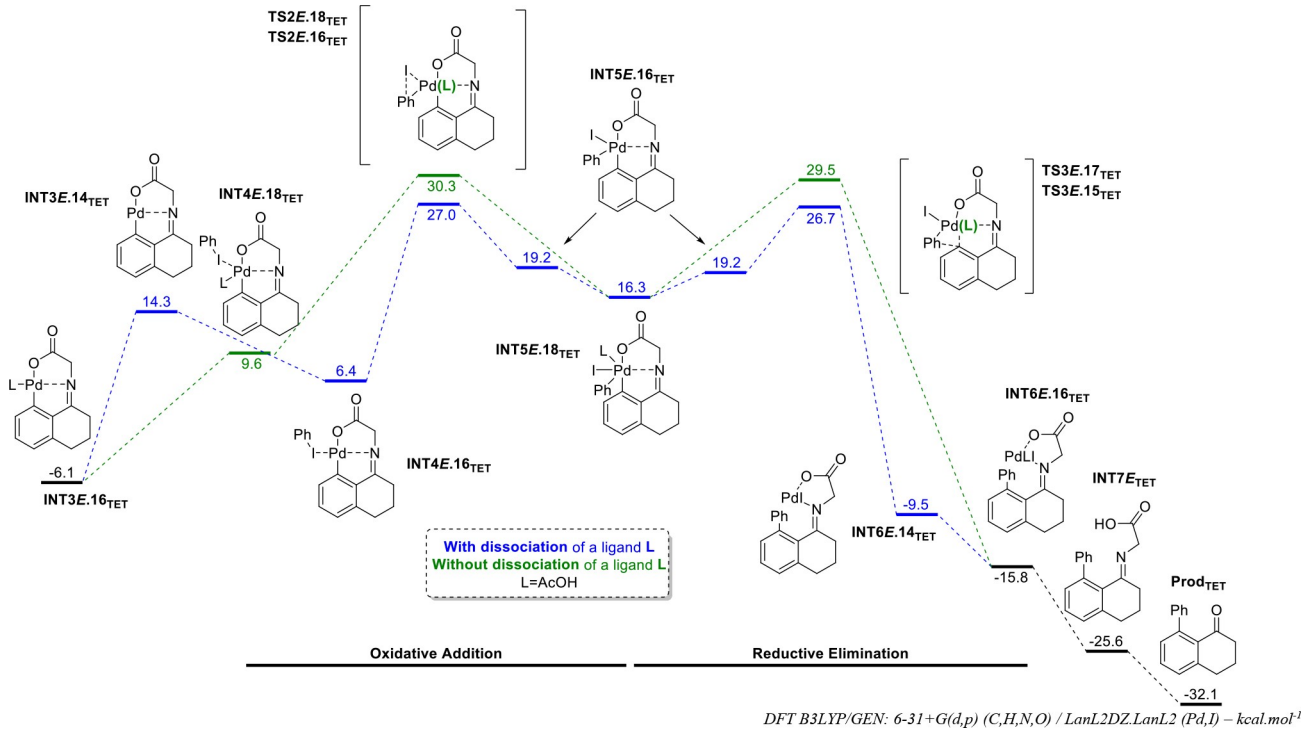

Figure 3. Energetics of reaction coordinates for steps D and E with tetralone as reference (0 kcal.mol^{-1}).

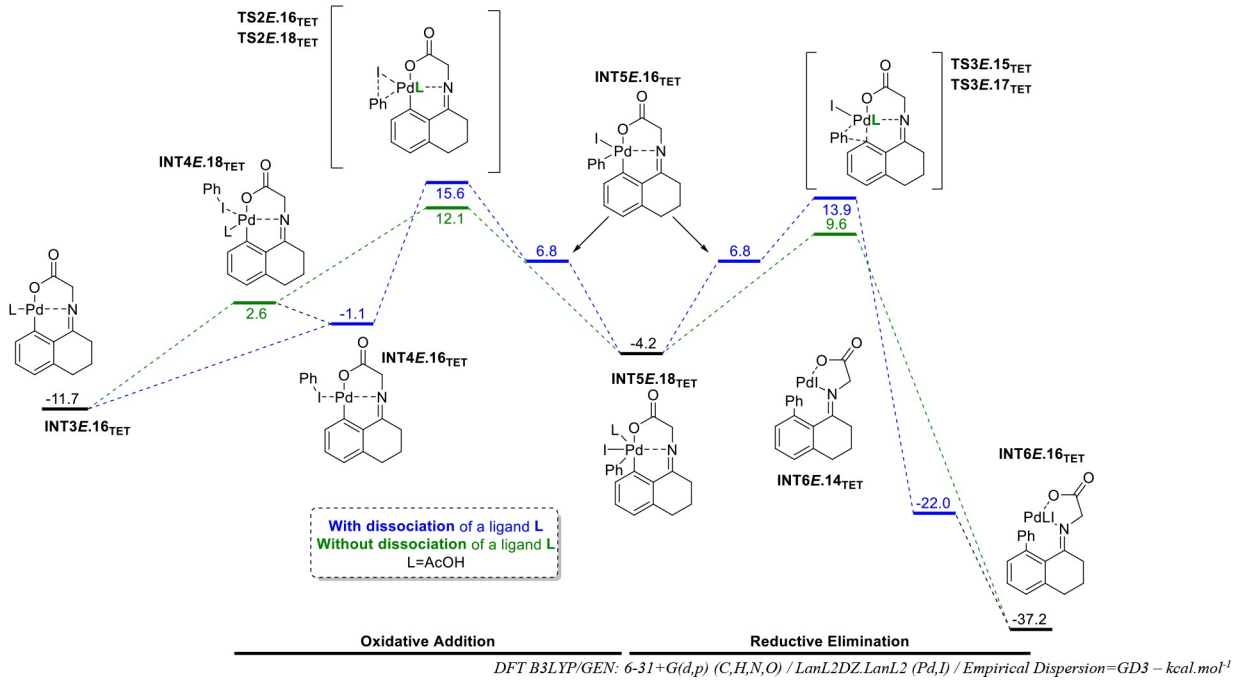

Figure 4. Energetics of reaction coordinates for steps D and E with tetralone as reference (0 kcal.mol^{-1}). Dispersion included.

influence of the presence and the size of the aliphatic ring on the outcome of the reaction. The results obtained are gathered in Figure 5. Interestingly, the early steps of the process leading to **INT2*E*.16** evidence that the successive formation of the tDG and the coordination to palladium required more energy in the case of tetralone (in green) than the corresponding acetophenone (blue) and benzo-fused cycloalkanones (orange and red). Each single step from the starting material highlights the particular behavior of tetralone. The higher energy required in these steps potentially indicates that the formation and the early reactivity of the tDG are crucial issues to address.

Further, activation of the C–H bond by Pd towards **INT3*E*.16** via **TS1*E*.16** resulted in a contrasted assessment. Indeed, indanone and benzosuberone required the highest amount of energy (barriers of 25.2 and 23.8 kcal.mol^{-1} respectively). Tetralone and acetophenone required less energy (barriers of 17.8 and 19.8 kcal.mol^{-1} respectively) for the corresponding step. In addition, **INT3*E*.16** appears the most favored for acetophenone and in decreasing order for tetralone, benzosuberone and indanone likely as a consequence of less crowded metallacycle. The following main intermediates and transition states until the reductive elimination **TS3*E*.15**, are illustrative of a similar trend in which indanone intermediates are always the more energetic, followed by benzosuberone, tetralone and acetophenone.

The reductive elimination step via **TS3*E*.15**, allows splitting two sets of substrates based on the energy of their respective TS: indanone and suberone with highest energy barriers and acetophenone and tetralone with lowest barriers. Finally, the formation of the C–C bond followed by regeneration of the carbonyl moiety led to the arylation products. Small energetic differences can be observed at this stage which take into account (i) the increase of the steric crowding around the newly created C–C bond (ii) the favorable energy release occurring from the palladacycle ring opening and thus favor the less crowded aryl indanone and aryl acetophenone rather than the tetralone and benzosuberone analogues.

Our calculations and comparison of overall energetic profiles within the benzo-fused cycloalkanone series show that the arylation is thermodynamically favored by 35.8 to 32.1 kcal.mol^{-1} from the starting materials to the products. Arylation of tetralone is the most favored process in all critical steps from the C–H activation (step C). The rather high energetic profile of early steps including formation of the tDG and coordination to Pd, might however hamper the progress of the arylation of tetralone. Unless late stage of the process, the presence of a cycloalkanone ring imparts additional stiffening in key intermediates and TS and thus results higher energetic profiles by comparison with acetophenone. Including the dispersion in theses calculation did not change the overall conclusion of this study – The reaction is more favored when using acetophenone as substrate, followed by benzotetralone, benzosuberone, and finally indanone, which does not react in these conditions. The complete

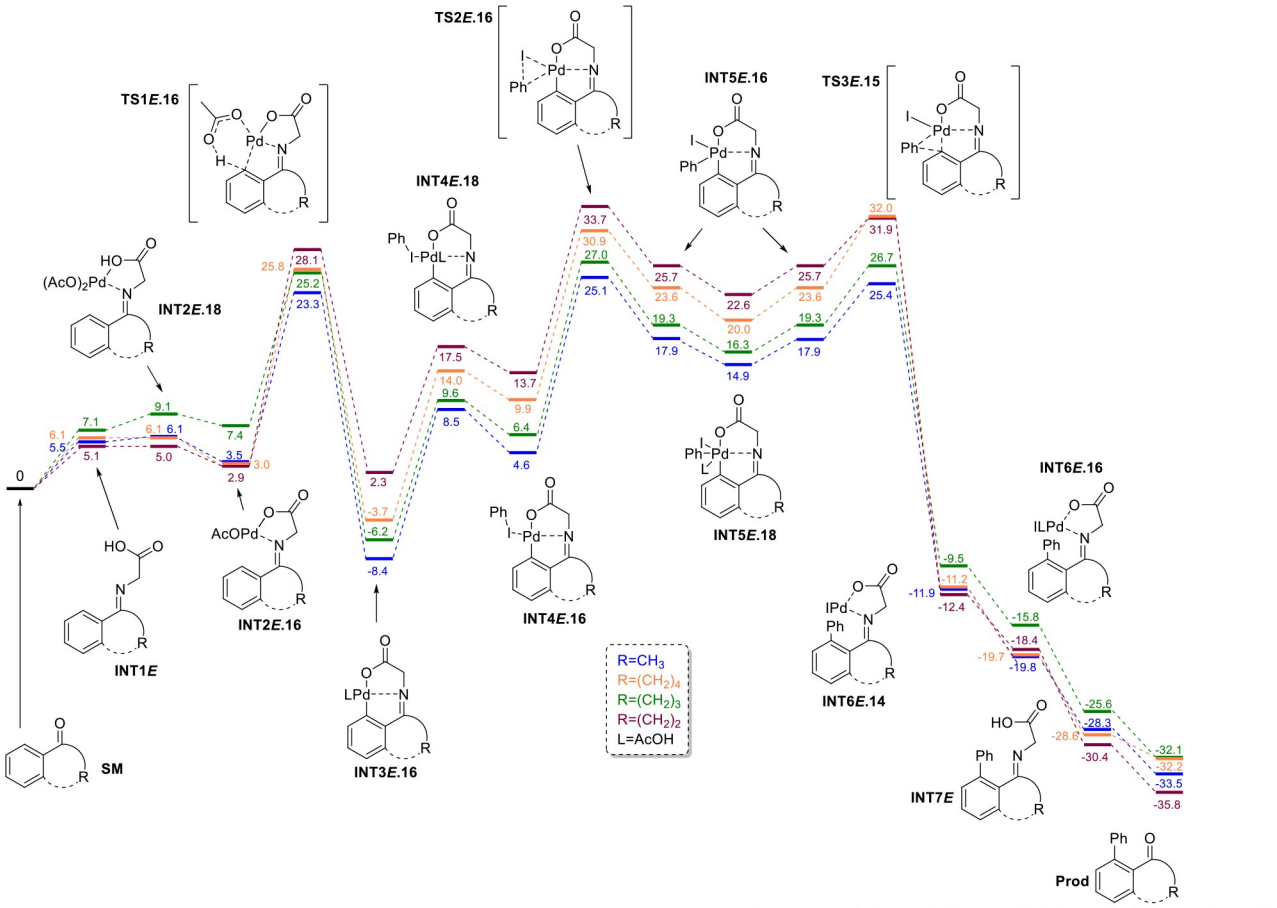

Figure 5. Comparison of energetic profiles for tetralone, acetophenone, benzosuberone and indanone.

energetic pathway, including this parameter, can be found in ESI.

Careful examination of the topology of each calculated intermediate or TS palladacycle showed that the variation of the energetic profiles observed by comparing acetophenone and members of the benzo-annulated cycloalkanone family is consistent with key structural features such as bond distances and angles within the different palladacycles (from **TS1*E*.16** to **TS3*E*.15**). In our analysis, distances and angles measured for the acetophenone-based intermediates have been considered as standard (Figure 6 & ESI). As exemplified in Figure 6, deviation and deformation from these standard values have been calculated for **INT3*E*.16$_{tet}$**, **INT3*E*.16$_{sub}$** and **INT3*E*.16$_{ind}$** which stand for the corresponding intermediates in the profiles of tetralone, suberone and indanone derivatives respectively (for a full analysis see ESI). For all bond distances and angles, values related to the indanone analogue are the most strongly deviated. In contrast, values related to the tetralone analogues are closest to standard.

In fact, the mean relative deformation of palladacycles within the benzo-fused cycloalkanones series allowed ranking indanone as the most distorted (2.4% of relative deformation), followed by benzosuberone (1.1% of relative deformation) and finally tetralone (0.3% of relative deformation). The deformation trend observed further questioned about the structure-reactivity relationship within this series of substrate. We thus started to experimentally evaluate the propensity of each member of the benzo-fused cycloalkanone family to undergo C–H arylation.

Optimization of the Reaction Conditions

We started to examine the C–H arylation on tetralone. First arylation attempts were based on experimental conditions recently reported by Jin.[17] Unfortunately, under these conditions a poor conversion was observed and only 11% of the expected compound has been isolated (Table 1 – Entry 1). A wide array of directing groups, palladium pre-catalysts, additives and solvents have been thoroughly screened (see Table 1 and ESI for full optimization tables) to determine the best

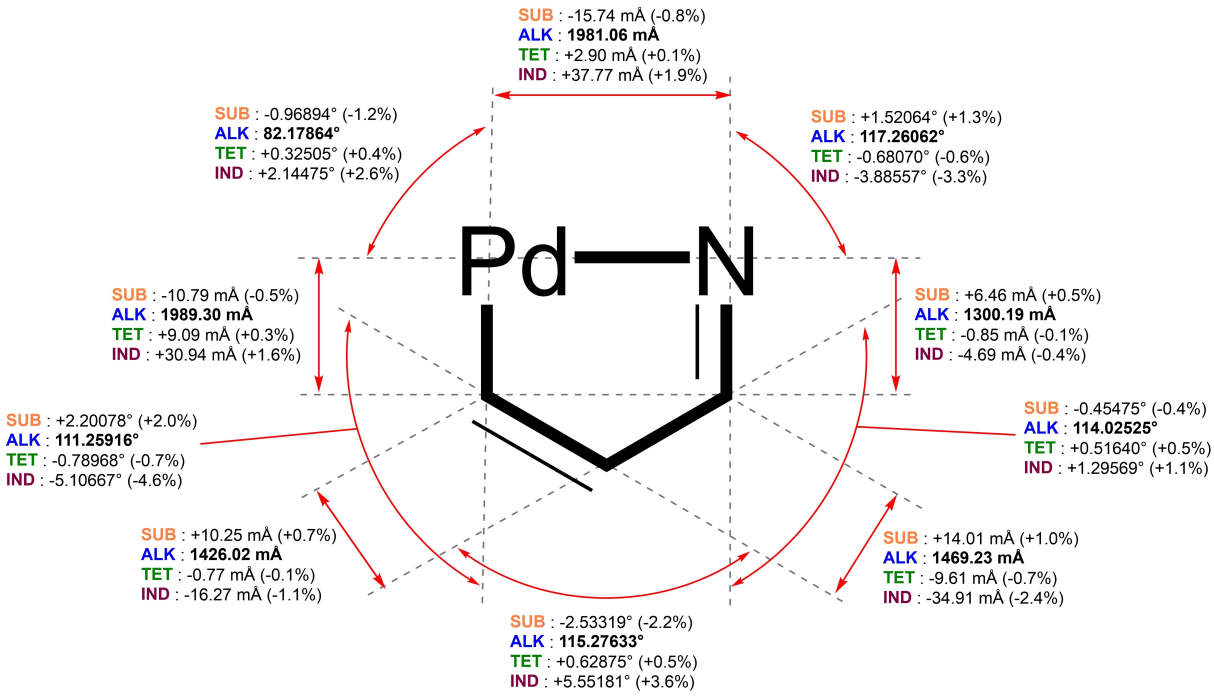

Figure 6. Palladacycle deformation for INT3E.16.

Table 1. Optimization of the experimental conditions.

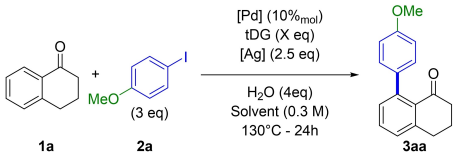

Entry	tDG	[Pd]/[Ag]	Solvent	3aa/1a
1	Gly (50%)	$Pd(PPh_3)_2Cl_2$/AgOAc	HFIP/AcOH (9/1)	1/4.6
2	Orthanilic acid (50%)	$Pd(PPh_3)_2Cl_2$/AgOAc	HFIP/AcOH (9/1)	1/10.2
3	Gly (50%)	$Pd(TFA)_2$/AgTFA	HFIP/AcOH (9/1)	1/1.2
4	Gly (50%)	$Pd(OAc)_2$/AgOAc	HFIP/TFA (9/1)	1/7.0
5	Gly (50%)	$Pd(OAc)_2$/AgOAc	AcOH	1/4.9
6	Gly (1 eq)	$Pd(TFA)_2$/AgTFA	HFIP/AcOH (9/1)	4.2/1

Ratio determined via NMR.

experimental procedure to perform this reaction. Our tests concluded that glycine was the most efficient tDG for this transformation (Table 1 – Entry 2). However, the more electrophilic [$Pd(TFA)_2$/AgTFA] catalytic combination (Table 1 – Entry 3) revealed more adapted for the arylation of tetralones than the classical [$Pd(PPh_3)_2Cl_2$/AgOAc] combination usually used to perform similar transformation on non-cyclic benzoalkanones. In addition, the arylation of tetralone appeared very sensitive to pH variation. Indeed, both the nature and the concentration of the acid co-solvent used to promote the formation of the transient imine were crucial parameters of this reaction (Table 1 – Entry 4 & 5). Strong Bronsted acids completely inhibit the reaction, and using weaker acid did not improve the **1a**/**3aa** ratio. The number of equivalents of glycine was next carefully examined. Under our conditions the use of a stoichiometric amount of glycine was essential to ensure highest conversion of the starting material (Table 1 – Entry 6), in good agreement with the aforementioned theoretical calculations. Indeed, the intermediates **INT1**, **INT2*E*.18** and **INT2*E*.16** were found to be less stable in the tetralone series than in the corresponding acetophenone series.

More importantly, attempts to use larger amount of glycine inhibits the reaction. Performing this reaction at a higher temperature or during an extended period of time did not improve the conversion either. Finally, the optimal conditions were defined as described in Table 1 (Entry 6).

Scope of the Reaction

The next step was dedicated to the extension of the scope of the reaction. We first applied the optimized conditions to indanone, tetralone and benzosuberone (Scheme 2).

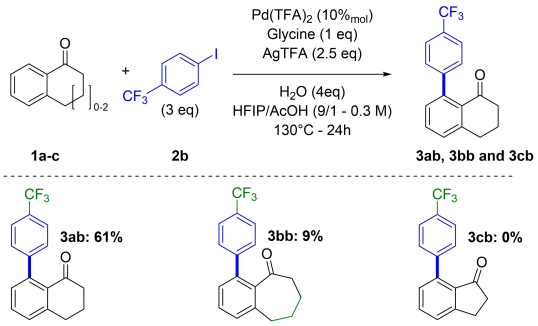

Scheme 2. Influence of the cycloalkanone ring size on arylation process.

While arylated tetralone **3 ab** could be isolated in 61% yield, benzosuberone derivative **3 bb** was obtained in 9% yield and the expected arylated indanone **3 cb** was not observed. These results and the trend observed experimentally are in complete adequacy with the calculated energetic profiles and the degree of deformation of key palladacycle intermediates.

To further widen the scope of this transformation, we performed this reaction with various aryl iodides (Scheme 3) on diverse tetralone derivatives (Scheme 4).

As expected, aryl iodides bearing electro-withdrawing groups were more easily coupled with tetralone derivatives under these conditions, as 61% of compounds **3 ab** have been isolated. Nitro groups (**3 ap**&**3 aq**) and esters (**3 ac**&**3 ak**) are also reasonably tolerated but the yield dropped when using an unprotected carboxylic acid (**3 ae**). Delightfully, the reaction leads to a halogeno aryl tetralone (**3 ad**&**3 al**–**ao**) when performed with iodo halogeno aryl derivatives. The remaining halogen can be use in potential additional coupling reactions leading to extended architectures. Unfortunately, the arylation does not occur when using *ortho* substituted aryl iodides, or activated iodides. Most likely overcrowding the reaction site disfavors the formation of a Pd^{IV} intermediate complex at the oxidative addition stage. The reaction issue appears sensitive to the presence of a substituent near the reacting site: the yield decreases from 57% to 35% when the methoxy group is moved from position 5 (**3 db**) to position 6 (**3 eb**), and drops to 10% when this group is located on position 7 (**3 fb**). Again, this result is probably due to an increase of the steric hindrance disfavoring the formation of the Pd^{IV} intermediate (Figure 7).

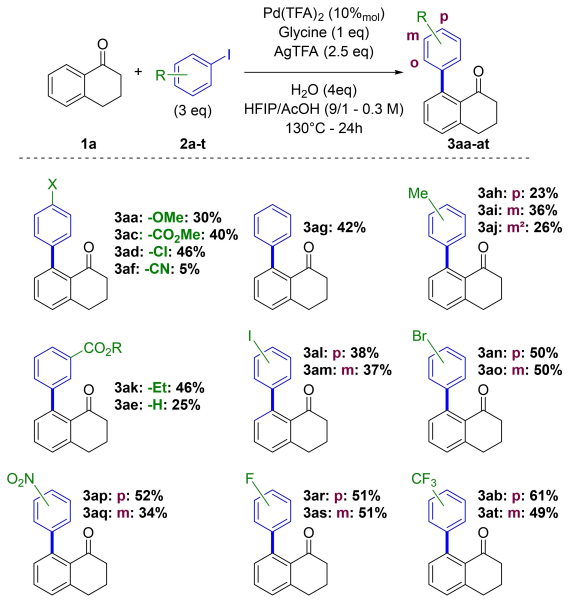

Scheme 3. Scope of the aryl iodides.

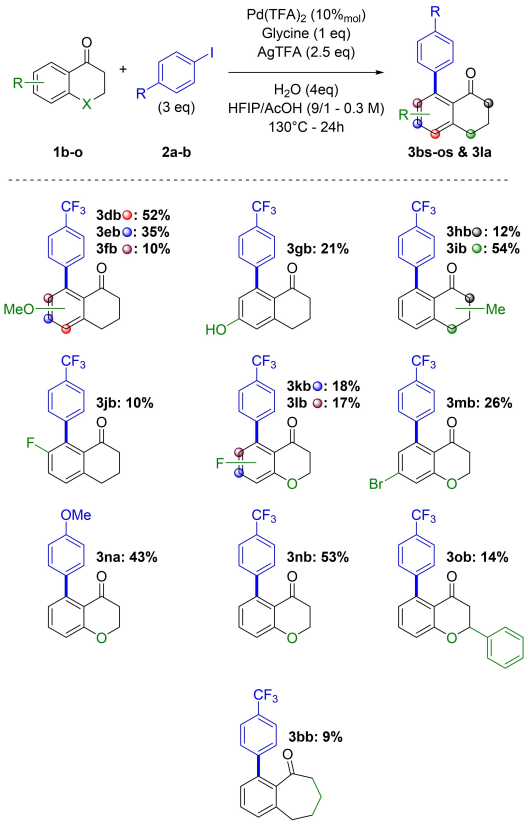

Scheme 4. Scope of benzocycloalkanones.

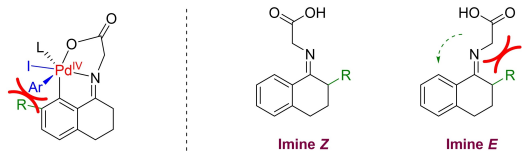

Figure 7. Impact of the steric hindrance over the Z to E imine intermediate.

The presence of an additional substituent close to the ketone function at the cycloalkanone ring also impacted the reaction outcome: 54% yield was obtained with a methyl group located at position 4 (**3 ib**) against 12% at position 2 (**3 hb**). The presence of such substituent most likely favors the formation of a *Z*-imine, which has been shown detrimental in the early stages of the process (Figure 7), according to our calculations (Figure 2). When the benzoalkanone derivative bears strong electron-donating substituents, the expected product is not observed.

Application of the Methodology to the Synthesis of Extended Polycyclic Architectures

Our next objective was to take advantage of the intact ketone fragment after the arylation process. At this stage, the remaining ketone moiety offers an appealing and straightforward transformable organic platform. We thus envision illustrating the development potential of our approach by an access to high value polycycles and naphthalene derivatives. The dihydronaphthtalene scaffold recently showed a strong ability to complex ions due to its topology and synergistic contribution of weak interactions.[42] Ketones **3 aa**, **3 db** and **3 ib** undergo alpha C_{sp2} arylation using o-iodobromobenzene and Pd-Xantphos as the catalytic system to afford in one step new dihydronaphthobenzofuranes (Scheme 5).

Aryl ketones **3** can also be considered as advanced precursors of naphthalenes. C–H arylation of position 8 of naphthalene substrates usually requires the presence of elaborated directing groups. Our strategy represents an alternative to such methods and a new synthetic sequence towards polycyclic naphthalene-based derivatives. Oxidation of ketone **3 ab** into 8-arylnaphthol **5 ab**, followed by condensation with methylpent-enal afforded aryl naphthochromene **6 ab** in 56% yield using a known procedure (Scheme 6).[43]

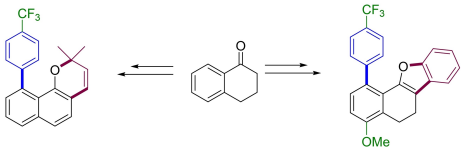

Scheme 5. Synthesis of dihydronaphthobenzofuranes & naphthochromenes.

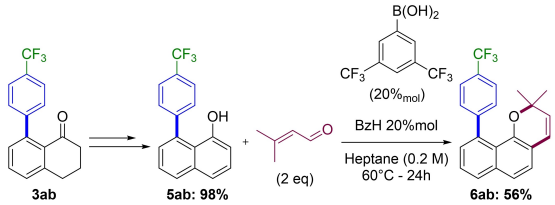

Scheme 6. Synthesis of aryl naphthochromene 6ab.

Conclusion

We explored the C–H arylation process of benzo-fused cycloalkanones through computational and experimental methods. Our theoretical study evidenced that both the presence and the size of the cycloalkanone ring deeply impact the outcome of the arylation sequence by comparison with classical acetophenone derivatives. Energetic profiles undoubtedly showed that the formation of imine derivatives to generate the tDG in early stages of the process is crucial. First the *E* imine is preferred over the *Z* imine in all cases. The formation of the *E* imine as well as successive elementary steps before the C–H activation step required higher energy for tetralone by comparison to other substrates, which is in good agreement with the mandatory use of stoichiometric amount of glycine to ensure high conversions. In contrast, in key oxidative addition and reductive elimination steps, the tetralone intermediates and transition states are clearly favored by comparison with suberone and indanone analogues. Our computational study also revealed that the topology of palladacycles involved in each step of the mechanism is a crucial parameter for C–H arylation. Analysis of bond distances and angles allowed determining a mean deformation of palladacycles and ranking indanone, suberone and tetralone from the most to the less distorted scaffold respectively. The deformation of intermediate palladacycles has been correlated to the reactivity trend within the benzo-fused cycloalkanones series. Indeed, under an optimized set of conditions, using glycine to generate the tDG, arylation of tetralone was readily obtained. In contrast, aryl benzosuberone was isolated with a poor yield and aryl indanone could not be obtained. A wide panel of diversely substituted aryl tetralones has been successfully synthesized, isolated and characterized with yields up to 61%. In addition, our strategy based on the sequential C–H arylation and further beneficial transformation of the residual ketone fragment, led to a straightforward alternative access to polycyclic architectures including polysubstituted naphthalene-based derivatives.

Experimental Section

General Procedure for the Arylation of Tetralone Derivatives

In a 2-dram screw glass tube, tetralone (1.0 eq) was added to a solution of glycine (1.1 eq), silver trifluoroacetate (2.5 eq), palladium acetate (0.1 eq) and aryl iodide (3.0 eq) and water (4.0 eq) in a mixture of HFIP and AcOH (9/1–0.3 M). The reaction mixture was stirred for 30 min at room temperature,

and for 24 h at 130 °C. After cooling to room temperature, the crude mixture was filtered through a pad of Celite, and purified using preparative TLC to obtain the desired product.

General Procedure for the Synthesis of Hydrazone Derivatives

In a round bottom flask, hydrazine (1.0 eq) was added to a solution of indanone (1.0 eq) in ethanol (0.5 M) and then stirred at room temperature for 17 h. The crude mixture was filtered over a no 4 fritted glass. The resulting solid was washed with ethanol to recover a part of the desired product. The combined liquids were concentrated over reduced pressure and purified using preparative TLC to retrieve the remaining desired compound.

General Procedure for the Synthesis of Dihydronaphthobenzofuranes Derivatives

Arylated tetralone (1.2 eq), Pd_2dba_3 (0.1 eq), cesium carbonate (3.0 eq) and Xantphos (0.24 eq) were placed in a 2-dram screw glass tube and left in a desiccator overnight. The tube was then filled with argon and a solution of aryl iodide (1.0 eq) in anhydrous toluene (0.7 M) was added. The resulting mixture was stirred for 5 days at 120 °C, diluted in AcOEt, filtered through a pad of Celite and purified using preparative TLC to afford the desired compound.

Acknowledgements

The Universities of Versailles St-Quentin and Paris-Saclay, the French Ministry of Superior Education and Research (PhD fellowship BL), and the CNRS are gratefully acknowledged for their financial support. This work was also supported by the French National Research Agency under the program CHARMMMAT ANR-11-LABX-0039-grant. This work was granted access to the computing resources of CINES (Montpellier, allocation A0060810812 awarded by GENCI).

References

[1] R. Manikandan, M. Jeganmohan, *Chem. Commun.* **2017**, *53*, 8931–8947.
[2] Z. Huang, J.-P. Lumb, *ACS Catal.* **2018**, *9*, 521–555.
[3] Y. Park, Y. Kim, S. Chang, *Chem. Rev.* **2017**, *117*, 9247–9301.
[4] P. Gandeepan, T. Müller, D. Zell, G. Cera, S. Warratz, L. Ackermann, *Chem. Rev.* **2019**, *119*, 2192–2452.
[5] K. Chen, X. Lei, *Curr. Opin. Green Sustain. Chem.* **2018**, *11*, 9–14.
[6] M. T. Mihai, G. R. Genov, R. J. Phipps, *Chem. Soc. Rev.* **2018**, *47*, 149–171.
[7] J. Yang, *Org. Biomol. Chem.* **2015**, *13*, 1930–1941.
[8] S. R. Neufeldt, M. S. Sanford, *Acc. Chem. Res.* **2012**, *45*, 936–946.
[9] W. Wang, M. M. Lorion, J. Shah, A. R. Kapdi, L. Ackermann, *Angew. Chem. Int. Ed.* **2018**, *57*, 14700–14717.
[10] M. Murai, K. Takai, *Synthesis* **2019**, *51*, 40–54.
[11] X.-Y. Chen, S. Ozturk, E. J. Sorensen, *Org. Lett.* **2017**, *19*, 6280–6283.
[12] D.-Y. Wang, S.-H. Guo, G.-F. Pan, X.-Q. Zhu, Y.-R. Gao, Y.-Q. Wang, *Org. Lett.* **2018**, *20*, 1794–1797.
[13] X. Y. Chen, S. Ozturk, E. J. Sorensen, *Org. Lett.* **2017**, *19*, 1140–1143.
[14] Z. Guan, S. Chen, Y. Huang, H. Yao, *Org. Lett.* **2019**, *21*, 3959–3962.
[15] X.-Y. Y. Chen, E. J. Sorensen, *J. Am. Chem. Soc.* **2018**, *140*, 2789–2792.
[16] X. H. Liu, H. Park, J. H. Hu, Y. Hu, Q. L. Zhang, B. L. Wang, B. Sun, K. S. Yeung, F. L. Zhang, J. Q. Yu, *J. Am. Chem. Soc.* **2017**, *139*, 888–896.
[17] J. Xu, Y. Liu, Y. Wang, Y. Li, X. Xu, Z. Jin, *Org. Lett.* **2017**, *19*, 1562–1565.
[18] D. Prim, S. Marque, A. Gaucher, J.-M. Campagne, in *Org. React.*, John Wiley & Sons, Inc., Hoboken, NJ, USA, **2011**, pp. 49–280.
[19] A. Izumoto, H. Kondo, T. Kochi, F. Kakiuchi, *Synlett* **2017**, *28*, 2609–2613.
[20] F. Kakiuchi, Y. Matsuura, S. Kan, N. Chatani, *J. Am. Chem. Soc.* **2005**, *127*, 5936–5945.
[21] T. Yamamoto, T. Yamakawa, *RSC Adv.* **2015**, *5*, 105829–105836.
[22] Y. Ogiwara, M. Miyake, T. Kochi, F. Kakiuchi, *Organometallics* **2017**, *36*, 159–164.
[23] F. Kakiuchi, Y. Matsuura, S. Kan, N. Chatani, *J. Am. Chem. Soc.* **2005**, *127*, 5936–5945.
[24] K. Kitazawa, T. Kochi, F. Kakiuchi, in *Org. Synth.*, John Wiley & Sons, Inc., Hoboken, NJ, USA, **2010**, pp. 209–217.
[25] D. Prim, D. Joseph, G. Kirsch, *Liebigs Ann.* **1996**, *1996*, 239–245.
[26] M. Wetzel, S. Marchais-Oberwinkler, R. W. Hartmann, *Bioorg. Med. Chem.* **2011**, *19*, 807–815.
[27] A. K. Macharla, R. Chozhiyath Nappunni, M. R. Marri, S. Peraka, N. Nama, *Tetrahedron Lett.* **2012**, *53*, 191–195.
[28] S. J. Gould, X. Cheng, C. Melville, *J. Am. Chem. Soc.* **1994**, *116*, 1800–1804.
[29] A. M. Bender, N. W. Griggs, C. Gao, T. J. Trask, J. R. Traynor, H. I. Mosberg, *ACS Med. Chem. Lett.* **2015**, *6*, 1199–1203.
[30] S. Zhu, Y. Xiao, Z. Guo, H. Jiang, *Org. Lett.* **2013**, *15*, 898–901.
[31] K. Sakthivel, K. Srinivasan, *J. Org. Chem.* **2014**, *79*, 3244–3248.
[32] S. Ponra, M. R. Vitale, V. Michelet, V. Ratovelomanana-Vidal, *J. Org. Chem.* **2015**, *80*, 3250–3257.
[33] S. Suzuki, K. Itami, J. Yamaguchi, *Angew. Chem. Int. Ed.* **2017**, *56*, 15010–15013; *Angew. Chem.* **2017**, *129*, 15206–15209.
[34] Y. Nakakuki, T. Hirose, H. Sotome, H. Miyasaka, K. Matsuda, *J. Am. Chem. Soc.* **2018**, *140*, 4317–4326.
[35] S. Makar, T. Saha, S. K. Singh, *Eur. J. Med. Chem.* **2019**, *161*, 252–276.

[36] S. Oi, S. Watanabe, S. Fukita, Y. Inoue, *Tetrahedron Lett.* **2003**, *44*, 8665–8668.
[37] R. B. Bedford, M. E. Limmert, *J. Org. Chem.* **2003**, *68*, 8669–8682.
[38] X. Tan, B. Liu, X. Li, B. Li, S. Xu, H. Song, B. Wang, *J. Am. Chem. Soc.* **2012**, *134*, 16163–16166.
[39] P. Gandeepan, L. Ackermann, *Chem* **2018**, *4*, 199–222.
[40] N. Thrimurtulu, A. Dey, A. Singh, K. Pal, D. Maiti, C. M. R. Volla, *Adv. Synth. Catal.* **2019**, *361*, 1441–1446.
[41] T. Bhattacharya, S. Pimparkar, D. Maiti, *RSC Adv.* **2018**, *8*, 19456–19464.
[42] H. Boufroura, S. Poyer, A. Gaucher, C. Huin, J.-Y. Salpin, G. Clavier, D. Prim, *Chem. Eur. J.* **2018**, *24*, 8656–8663.
[43] V. Dimakos, T. Singh, M. S. Taylor, *Org. Biomol. Chem.* **2016**, *14*, 6703–6711.

